ELSEVIER

Catalysis Today 50 (1999) 637–650

CATALYSIS TODAY

Diffusion and reaction in ZSM-5 and composite catalysts for the methanol-to-olefins process

Frerich J. Keil*, Jürgen Hinderer, Abdul R. Garayhi

Department of Chemical Engineering, Technical University of Hamburg-Harburg, Eissendorfer Str. 38, D-21073, Hamburg, Germany

Abstract

Diffusion and reaction in composite catalyst particles were calculated using the dusty-gas-model, Monte Carlo and Molecular dynamics calculations for the determination of multicomponent diffusivities of molecules participating in the methanol-to-olefins synthesis. A three-dimensional model of zeolite structures is presented. Without a fitting parameter, the diffusivities calculated in silicalite give a good approximation to the experimental data. Diffusion and reaction of the MTO synthesis is described with a model employing about 4000 particles. © 1999 Elsevier Science B.V. All rights reserved.

Keywords: ZSM-5; Methanol-to-olefin process; Composite catalysts

1. Introduction

Composite catalysts consist of small catalytically active particles that are embedded in an effectively inert matrix. Composite catalytic particles have become of increasing industrial importance over the last few years as they offer a number of advantages:

- In fluidized bed reactors, for example, attrition can be minimized by suitable preparation of the amorphous matrix. As most zeolites can so far only be synthesized of diameters of only a few micrometers, a loss of fine particles by elutriation can be almost entirely avoided.
- For deactivation due to blocking of channels or pore mouths, the operating life of composite catalysts is extended due to the slower clogging of macropores in the amorphous matrix. As a result, the reactants have access to the most of the embedded active catalyst particles for a longer period. The selectivity may thus also be improved.

Ruckenstein [28] first considered the advantages of embedding small catalyst particles uniformly within an inert porous matrix. As the diffusivities of molecules moving within the active catalyst (e.g. zeolites) are often very small, the effectiveness of the catalyst is correspondingly small for large homogeneous catalyst pellets. A smaller-sized pellet increases the effectiveness, but physical constraints may require a minimum size. Introducing small particles of active catalyst into an inert or less-active porous solid with a rather large pore diameter leads to a higher average diffusivity. This is the underlying concept of a composite catalyst. Varghese and Wolf [38] analyzed pore-mouth poisoning in the diluted composite catalyst and could show that the increased diffusivity of the inert matrix and its poison-jetter capacity can increase catalyst lifetime

*Corresponding author. Tel.: +49-40-42878-3042; fax: +49-42878-2145; e-mail: keil@tu-harburg.de

0920-5861/99/$ – see front matter
PII: S0920-5861(98)00498-2

and save on the active material required. Dadyburjor [5] found that an optimum distribution of the active component in the catalyst pellet may lead to significantly higher reaction rates per unit volume of pellet compared with reaction rates using pellets having a uniformly distributed active component. The optimum distribution changes qualitatively with the physical parameters of the pellet and with changes in the rate constants and diffusion coefficients of the catalytic components. Similar results were found by Lee and Ruckenstein [18]. Dadyburjor [6] and Lee and Ruckenstein [18] have studied the selectivity of composite pellets for first-order parallel and series types of reactions for different distributions of the active phase. ''Constrained'' optimal distributions of the more active phase in the less active matrix are obtained in every case. Dean and Dadyburjor [7] have experimentally investigated the deactivation of a composite acid catalyst during cracking of *n*-hexadecane by using a thermogravimetric analysis system operating as a pulse microreactor followed by a gas chromatograph. They found that the composite cracking catalyst exhibits advantageous behavior with respect to coke deactivation. Smirniotis and Ruckenstein [30] examined the performance of composite spherical or cylindrical single pellets containing ZSM-5 particles uniformly distributed in amorphous silica–alumina for catalytic cracking of *n*-hexane.

The reactant cracking was assumed to obey first-order irreversible kinetics. Steady-state analytical solutions for the concentration profiles of the reactant, the effectiveness factor for the pellets, and the yields of the produced species were calculated. This model has also been used by Hinderer and Keil [12]. In the above mentioned papers the diffusivities, especially in zeolites, could only be calculated approximately. Although reaction schemes were considered which entailed changes of the reactant volumes, this was not taken into account in the models used. Modeling of composite particles leads to the following problems among others:

- The need to describe multicomponent diffusion and reaction within the amorphous matrix.
- Intracrystalline diffusion within the zeolite (or other) microporous particles has to be calculated.
- In some cases, surface barrier resistance through the outer layer of the zeolite crystals has to be considered. Film resistance around the pellets may also be involved.

Concerning the amorphous matrix, molecular diffusion, Knudsen diffusion, and surface diffusion have to be taken into consideration. The dusty-gas-model is a suitable approach for this purpose. Mason and Malinauskas [22] give a clear presentation of this model. The problem of multicomponent diffusion is outlined in a book from Taylor and Krishna [32] and in a recently published review by Krishna and Wesselingh [16] (see also [15]). The intracrystalline diffusion in zeolites is dominated by the continuous interaction of the sorbate molecules with the walls of the adsorbent. As the pore diameters within zeolites are similar to the molecular dimensions, distinctions between gas and condensed phases lose their meaning. The electrons of the molecules overlap strongly with electrons of the zeolite oxygen atoms. Therefore, a full understanding of the details of diffusion within zeolites (''configurational diffusion'') will only be possible with the aid of quantum mechanics, statistical physics and appropriate experimental methods. Reasonably good results have been obtained by using approximate interaction potentials. Molecular dynamics (MD), Monte Carlo calculations (MC), transition-state theory computations (TST) and Brownian dynamics approaches (BD) are the prevailing methods employed to describe the ''configurational diffusion''. Reviews are presented in books by Kärger and Ruthven [14], Chen et al. [4], and in papers written by Demontis and Suffritti [8], Theodorou et al. [34], and van Santen et al. [35], among others. A compilation of experimental methods is given by Post [25] and Rees [26].

Theodorou and Wei [33] first developed a Monte Carlo approach to simulate intracrystalline diffusion and reaction in a ZSM-5 crystallite. Binary diffusion components and the xylene isomerization were calculated by Frank et al. [9]. Wang et al. [40,41] simulated the isomerization reaction of xylene and the alkylation of toluene with alcohols by means of the MC method based on experimentally observed parameters, including the diffusivity, equilibrium adsorption constant, and intrinsic rate constant. Besides the MC approach, a variety of MD calculations has been carried out [34]. The most recent method was published by Maginn et al. [20]. Their simulation strategy utilizes concepts

from Brownian motion theory and transition-state theory and can be used to determine diffusivities for chains of up to C_{20} using modest computational resources.

The present paper focuses on the following points:

- Multicomponent diffusion and reaction in composite catalysts is modeled. The methanol-to-olefins synthesis (MTO) is taken as an example.
- In contrast to previous publications, a volume change during the reaction is taken into account.
- Any common chemical kinetics may be employed.
- The multicomponent fluxes within the amorphous matrix are described by the dusty-gas-model (DGM).
- Diffusivities within the microporous crystallites (e.g. zeolites) are modeled using a Monte Carlo (MC) approach. A very large number of particles and channel intersections within the zeolites is used. Several MD calculations are carried out for comparison.
- Reaction probabilities are introduced for the simulation of the MTO synthesis.

2. Theory

2.1. Composite catalyst particles

According to Ruckenstein [28], one can assume that diffusion and reaction in two phases, the catalytically active (e.g. zeolites) and the amorphous phase can be treated independently. The fluxes and the reaction rates are added to give the total flux, $\mathbf{j}_t$, and the total reaction rate, R_t:

$$\mathbf{j}_t = (1-\zeta)\cdot\mathbf{j}_m + \zeta\cdot\mathbf{j}_a \tag{1}$$

and

$$\mathrm{R}_t = (1-\zeta)\cdot\mathrm{R}_m + \zeta\cdot\mathrm{R}_a, \tag{2}$$

where $\mathbf{j}_a$ and $\mathbf{j}_m$ correspond to the mole fluxes within the active and the amorphous matrix phase, respectively. The term ζ represents the volume fraction of the active component, whereas R_m and R_a are reaction rates for the matrix and the amorphous phase. A schematic view of a composite particle is illustrated in Fig. 1. The material balance over a spherical shell

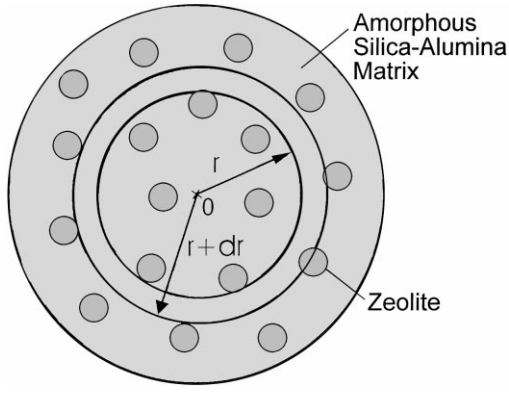

Fig. 1. Section of a spherical composite catalyst pellet.

of the pellet under steady-state conditions leads to

$$\begin{aligned}0 = {} & (1-\zeta)\cdot\mathbf{j}_m(r)\cdot A(r) - (1-\zeta)\cdot\mathbf{j}_m(r+\mathrm{d}r)\\ & \cdot A(r+\mathrm{d}r) + \zeta\cdot\mathbf{j}_a(r)\cdot A(r) - \zeta\cdot\mathbf{j}_a(r+\mathrm{d}r)\\ & \cdot A(r+\mathrm{d}r) + (1-\zeta)\cdot\sum_{i=1}^{n_r}\nu_i\cdot R_m(r)\cdot\mathrm{d}V + \zeta\\ & \cdot\sum_{i=1}^{n_r}\nu_i\cdot R_a(r)\cdot\mathrm{d}V\end{aligned} \tag{3}$$

$A(r)$ is the surface area of a sphere with a radius of r. The ν_i are the stoichiometric coefficients. The amorphous phase is described by the dusty-gas-model [22] since the pore radii of the pores are rather large so that molecular and/or Knudsen diffusion prevail. At higher pressures and with more polar components, surface diffusion becomes increasingly important. Volume changes during reaction or inconsistencies with Graham's law give rise to viscous' fluxes. According to the DGM fluxes, $\mathbf{j}$, are comprised additively of three parts

$$\mathbf{j} = \mathbf{j}^D + \mathbf{j}^S + \mathbf{j}^V, \tag{4}$$

where D, S and V represent the diffusive, surface and viscous fluxes, respectively. The surface diffusion in the amorphous phase was neglected in the present instance as the MTO reaction takes place at atmospheric pressure. The approach of Krishna [17] for the surface diffusion might have been used if this effect had been important. The viscous flow is approximated by Hagen–Poiseuille's equation

$$\mathbf{j}^V = -\mathbf{c}\frac{r_p^2}{8\eta}\frac{\mathrm{d}p}{\mathrm{d}r}, \tag{5}$$

where $\mathbf{c}$ is the concentration of reactive species, p the pressure, and η the viscosity of the gas mixture. By employing the following Taylor expansions to the first term and taking Eq. (4) into consideration, one finds for Eq. (3) that

$$0 = (1-\zeta)\left\{ -\left(\mathbf{j}_{\mathrm{m}}^{\mathrm{D}} + \mathbf{j}_{\mathrm{m}}^{\mathrm{S}} + \mathbf{j}_{\mathrm{m}}^{\mathrm{V}}\right)_r \cdot \frac{\mathrm{d}A}{\mathrm{d}r} \cdot \frac{1}{A(r)} - \frac{\mathrm{d}\left(\mathbf{j}_{\mathrm{m}}^{\mathrm{D}} + \mathbf{j}_{\mathrm{m}}^{\mathrm{S}} + \mathbf{j}_{\mathrm{m}}^{\mathrm{V}}\right)}{\mathrm{d}r} \cdot + \sum_{r=1}^{n_{\mathrm{r}}} \boldsymbol{\nu}_{\mathrm{jr}} \cdot R_{\mathrm{m,r}} \right\} + \zeta\left\{ -\mathbf{j}_{\mathrm{a}}^{\mathrm{D}} \cdot \frac{\mathrm{d}A}{\mathrm{d}r} \cdot \frac{1}{A(r)} - \frac{\mathrm{d}\mathbf{j}_{\mathrm{a}}^{\mathrm{D}}}{\mathrm{d}r} + \sum_{r=1}^{n_{\mathrm{r}}} \boldsymbol{\nu}_{\mathrm{jr}} \cdot R_{\mathrm{a,r}} \right\}. \quad (6)$$

One should bear in mind that the diffusivities for zeolites were taken from MC or MD calculations.The rate of reaction within the active component, R_{a}, can be calculated by means of an effectiveness factor of the active particles, φ^{a}, and the intrinsic rate of reaction, $R_{\mathrm{a}}^{\mathrm{int}}$:

$$R_{\mathrm{a}} = \varphi^{\mathrm{a}} R_{\mathrm{a}}^{\mathrm{int}}. \quad (7)$$

Within the amorphous matrix phase there is no further diffusion limitation, and all components have access to the actives sites. Eq. (6) thus yields

$$0 = \left[(1-\zeta)\left\{\mathbf{D}^{-1} + \mathbf{D}^{\mathrm{s}} + RT\frac{r_{\mathrm{p}}^2}{8\eta}\mathbf{c}\mathbf{e}^{\mathrm{T}}\right\} + \zeta\mathbf{D}_{\mathrm{eff}}^{\mathrm{a}}\right] \times \frac{\mathrm{d}^2\mathbf{c}}{\mathrm{d}r^2} + \left[(1-\zeta)\left\{\frac{2}{r}\left(\mathbf{D}^{-1} + \mathbf{D}^{\mathrm{s}} + RT\frac{r_{\mathrm{p}}^2}{8\eta}\mathbf{c}\mathbf{e}^{\mathrm{T}}\right) + \frac{\mathrm{d}\mathbf{D}^{-1}}{\mathrm{d}r} + RT\frac{r_{\mathrm{p}}^2}{8\eta}\frac{\mathrm{d}\mathbf{c}}{\mathrm{d}r}\mathbf{e}^{\mathrm{T}}\right\} + \frac{2}{r}\zeta\mathbf{D}_{\mathrm{eff}}^{\mathrm{a}}\right]\frac{\mathrm{d}\mathbf{c}}{\mathrm{d}r} + (1-\zeta)\sum_{i_{\mathrm{r}}=1}^{n_{\mathrm{r}}} \boldsymbol{\nu}_{i_{\mathrm{r}}} R_{\mathrm{m},i_{\mathrm{r}}} + \zeta\sum_{i_{\mathrm{r}}=1}^{n_{\mathrm{r}}} \boldsymbol{\nu}_{i_{\mathrm{r}}}\varphi^{\mathrm{a}} R_{\mathrm{a},i_{\mathrm{r}}}, \quad (8)$$

where

$$\mathbf{e}^{\mathrm{T}} = (1,1,1,\ldots,1), \quad (9)$$

$$\mathbf{D} = -\frac{x_i}{D_{ij}} - \sum_{\substack{l=1 \\ l\neq i}}^{N} \frac{x_l}{D_{il}} - \frac{1}{D_i^K} \quad |i \neq j, \quad \mathbf{D} = 0 \quad |i = j. \quad (10)$$

The corresponding boundary conditions are:

$$\mathbf{c}(R_0) = \mathbf{c}_{\mathrm{s}} \quad (11)$$

and

$$\left.\frac{\mathrm{d}\mathbf{c}}{\mathrm{d}r}\right|_{r=0} = 0. \quad (12)$$

Generally the concentrations at the surface, $\mathbf{c}_{\mathrm{s}}$, are unknown and quite often depend on external mass-transfer resistances. Therefore, the boundary condition in [8] is replaced by the equation

$$\mathbf{k}_{\mathrm{s}}(\mathbf{c}_{\mathrm{s}} - \mathbf{c}_{\mathrm{b}}) = (1-\zeta)\mathbf{j}_{\mathrm{m}}|_{r=R_0} + \zeta\mathbf{j}_{\mathrm{a}}|_{r=R_0}, \quad (13)$$

where $\mathbf{c}_{\mathrm{b}}$ represents the bulk concentration. For a rigorous solution, the effectiveness factor, φ^{a}, can be calculated from a boundary value system similar to Eqs. (8)–(13) with ζ=1. As these calculations would be very time consuming, the effectiveness factor approximated according to a first-order reaction without any volume change. A first-order reaction from the reaction scheme given below is taken as a key reaction

$$\varphi^{\mathrm{a}} = \frac{3}{\Phi_{\mathrm{a}}}\left[\frac{1}{\tanh(\Phi_{\mathrm{a}})} - \frac{1}{\Phi_{\mathrm{a}}}\right], \quad (14)$$

with the Thiele modulus of the active particles

$$\Phi_{\mathrm{a}} = r_0\sqrt{\frac{k_{\mathrm{a}}}{D^{\mathrm{a}}}}, \quad (15)$$

where k_{a} is the reaction rate constant and r_0 the radius of the active particle. The diffusivities within the zeolites were taken from Monte Carlo simulations as will be outlined below. At low Reynolds numbers, the mass transfer coefficient is difficult to determine [21]. For the case in hand examples the empirical correlation suggested by Kröger was used [2]:

$$\frac{Sh}{Re\,Sc^{1/3}}\frac{1}{0.12+\epsilon_{\mathrm{r}}} = \frac{3.72}{Re^{2/3}} + \frac{1.06}{30+Re^{1/3}}, \quad (16)$$

Sh, Re, Sc and ϵ_{r} are the Sherwood, Reynolds, Schmidt number and bed porosity, respectively. The $D_{\mathrm{eff}}^{\mathrm{a}}$ coefficients were taken from separate Monte Carlo calculations of single zeolite particles described in Section 3. These coefficients were put into Eq. (10).

For the MTO synthesis, the following reaction scheme published by Schönfelder et al. [29] was chosen

$$A \xrightarrow{k_1} B + W, \quad (17)$$

$$A + B \xrightarrow{k_2} C + W, \quad (18)$$

$$A + C \xrightarrow{k_3} D + W, \quad (19)$$

$$B \xrightarrow{k_4} \tfrac{2}{3}E, \quad (20)$$

$$C \xrightarrow{k_4} E, \quad (21)$$

$$D \xrightarrow{k_4} \tfrac{4}{3}E, \quad (22)$$

$$A \xrightarrow{k_5} \tfrac{3}{2}F + \tfrac{1}{2}W. \quad (23)$$

In this scheme, some of the species are lumped together: A (methanol and dimethylether), E (paraffins), and F (decomposition products). The remaining components are abbreviated by B (ethene), C (propene), D (butene) and W (water). All kinetic expressions were approximated to be of first-order with respect to the reactants.

The values of the rate constants were obtained from measurements in a Berty reactor at 773 K (Table 1).

The system of Eqs. (8)–(13) was solved by employing routines from the NAG (The Numerical Algorithms Group, Oxford, UK; Mark 17) library. The roots of the algebraic equations resulting from the boundary conditions were solved by a combined Powell-hybrid method (routine C05NDF). Two different methods were used to solve the boundary value problem, a shooting and matching technique (D02HAF), and a finite difference method (D02GAF).

3. Monte Carlo calculations of diffusivities in zeolites

Theodorou and Wei [33] studied the diffusion and simple isomerization reaction A⇔B in a regular pore network by use of a Monte Carlo method. The results revealed that MC simulations are an efficient and self-consistent approach for solving problems of diffusion and reaction in microporous solids. Various MC methods were employed by different research groups. June et al. [13] calculated Henry's constants and isosteric heats of sorption via the evaluation of configurational integrals with an MC integration scheme. The spatial distribution of sorbate molecules within the pore network, as well as perturbations to their conformation due to confinement in the pores, were determined with a Metropolis MC algorithm. Simulations of sorbate spatial distributions showed that linear alkanes such as *n*-butane and *n*-hexane, preferentially reside in the channels and avoid the channel intersections. Bulky side groups on the other hand force molecules to the channel intersections. Van Tassel et al. [37] calculated thermodynamic properties and density distributions of Xe atoms trapped in the alpha cage of zeolite NaA using the canonical ensemble MC technique to determine adsorption isotherms and isosteric heats of adsorption for benzene and *p*-xylene in silicalite. Predictions of adsorption isotherms, isosteric heats, and siting locations of the adsorbates are in good agreement with experiments. Maginn et al. [19] introduced a bias MC method to predict low-occupancy adsorption thermodynamics of *n*-alkanes ranging in length from C_4 to C_{25} in the zeolite silicalite. The idea behind the bias MC techniques is to generate chains according to a weight (bias) function such that the generated chains are ''threaded'' bond-by-bond through contiguous open or energetically favorable regions within the zeolite.

Table 1
Reaction rate constants

k_1	6.73×10^{-3} [m^3/(kg s)]
k_2	3.42×10^{-3} [m^6/(s kg mol)]
k_3	5.0×10^{-4} [m^6/(s kg mol)]
k_4	2.09×10^{-5} [m^3/(s kg)]
k_5	2.74×10^{-4} [m^3/(s kg)]

In the present paper, diffusion of molecules participating in the MTO synthesis in silicalite and their reaction steps will be treated by an MC approach. Firstly, the geometric structure has to be defined. Secondly, multicomponent diffusion of the reactants has to be calculated followed by the computation of the reaction. A short outline of the procedure has been described by Hinderer and Keil [11].

As the reaction within a zeolite is a ''rare event'', one needs a quite large lattice structure and a large number of particles in order to have a reasonable number of reaction events within a period of time using today's computer facilities. Calculating diffusivities by employing equilibrium MD simulations would take about 6000 h of Cray Y-MP time according to an estimate by Theodorou et al. [34]. Transition-

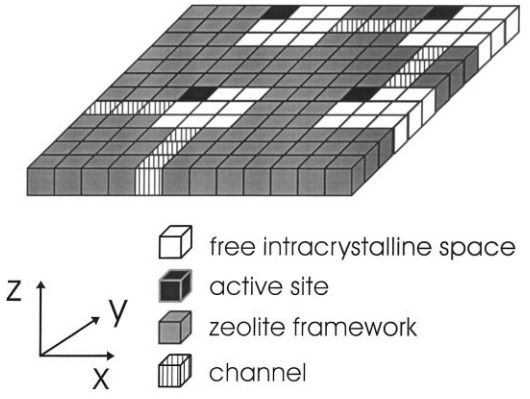

Fig. 2. Sectional plane of ZSM-5 as used for MC calculations.

state theory (TST) could be used instead of MC computations, but with multicomponent mixtures this remains a formidable task. Voter [39] has recently published a TST-based method for extending the MD timescale that does not require advanced knowledge of the states of the system or the transition states that separate them.

The present authors have modeled the ZSM-5 silicalite structure as a three-dimensional lattice consisting of four different types of lattice elements. A sectional plane is given in Fig. 2:

- a rigid zeolite framework which is impenetrable for molecules;
- intracrystalline space in which molecules can move;
- channels connecting the cages;
- active sites where molecules can adsorb and react.

With the aid of these elements, any size of a lattice can be generated by the periodic arrangement of lattice elements.

The present MC calculations are based on $96\times96\times96$ lattice elements resulting in 4096 channel intersections. Between one and six molecules per intersection were used. The position of the active centers and their number within a unit cell may be chosen. In order to avoid boundary effects, periodic boundary conditions were introduced (see e.g. [1]). The diffusive transport is modeled as a random walk process, i.e. a sequence of uncorrelated activated jumps of molecules in the lattice. Initially 4096 particles are randomly distributed over the three-dimensional network of channels and intersections. During one MC step, each molecule is chosen in a random sequence. If the movement of a certain molecule is possible in the direction chosen at random, the movement continues until the molecule collides with another molecule or the rigid zeolite framework. This reduces the jump probability in accordance with the number of molecules in the vicinity. It is then checked whether a molecule is too large to pass through a channel. If the saturation capacity of a channel or intersection is reached, no further molecules can occupy this channel or intersection. A molecule residing on an active site has to pass over a potential barrier (see below for details). Similarly, a channel intersection can be left only when the molecule overcomes a potential barrier. Pairwise additive intermolecular interactions among any type of sorbate molecule are taken into account. In order to keep the computation time at a reasonable level, the intermolecular interaction of sorbate molecules is just confined to that particular channel or intersection which is occupied by the same molecules. Chemical reactions can take place on active sites with a reaction probability to be specified. The program structure used to simulate the movement of molecules is given in Figs. 3 and 4. An important aspect is the interaction potentials. For the potential between the sorbate molecules and the oxygen atoms of the zeolite framework, the following sum of pairwise additive (12,6)-Lennard-Jones (LJ) potentials was used:

$$\Phi = \sum_{n_o} 4\epsilon \left[\left(\frac{\sigma}{r}\right)^{12} - \left(\frac{\sigma}{r}\right)^{6} \right], \tag{24}$$

where n_o corresponds to the number of interacting oxygen atoms, ϵ and σ are the LJ parameters. The distance between the nuclei of two particles is given by r. As the polarizability of silicon atoms is quite small and as the silicon atoms in silicalite are covered by oxygen atoms, the interaction between the sorbate molecules and the silicon atoms of the zeolite lattice is neglected. This assumption has been made by several authors in the past. The potential depends mainly on the zeolite geometry, number of oxygen atoms, and molecular dimensions. A channel in silicalite is surrounded by a 10-membered oxygen ring with the resulting potential

$$\Phi_C = \sum_{10} 4\epsilon_{ij} \left[\left(\frac{d_m + d_o}{d_c + d_o}\right)^{12} - \left(\frac{d_m + d_o}{d_c + d_o}\right)^{6} \right], \tag{25}$$

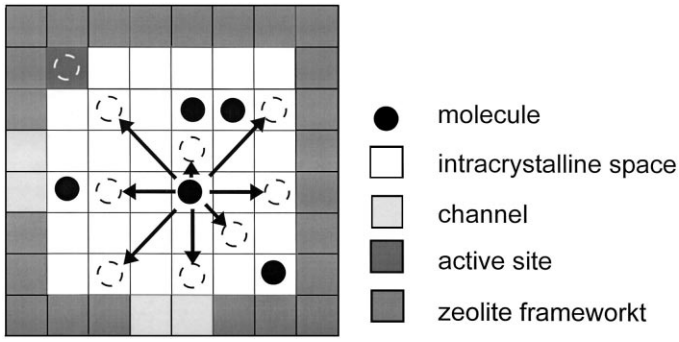

Fig. 3. Movements of molecules during MC calculations.

where the distance, r, from the center of the channel to the nuclei of oxygen atoms is calculated as

$$r = 0.5(d_c + d_o). \tag{26}$$

The diameter of the channel and the oxygen atom is represented by d_c and d_o, respectively. According to Xiao and Wei [42], d_o can be taken as 2.6 Å. For d_c, the present authors took the average channel size of 5.4 Å. The minimum kinetic diameter of the molecules is d_m. The values for d_m were taken from Breck [3]. The LJ-parameters can be estimated with the aid of semiempirical equations by Wilke and Lee which may be found in the book written by Reid et al. [27].

The values for ϵ_{ij} and σ_{ij} are based on the Lorentz–Berthelot mixing rules:

$$\sigma_{ij} = 0.5(\sigma_i + \sigma_j), \tag{27}$$

$$\epsilon_{ij} = \sqrt{\epsilon_i \epsilon_j}. \tag{28}$$

The effective diameter of the intersection, d_i, is approximately 8.7 Å. The values for ϵ_m were also taken from Breck [3]. One should bear in mind that neither the zeolite channel diameter nor the molecular diameter can be characterized by a precise number. The electron density distribution reaches its zero level only at infinity, but the density falls off very rapidly, so that only an approximate diameter can be assumed. Furthermore, molecular vibrations and rotations as well as lattice vibrations make it difficult to assess a diameter for either molecule or zeolite pore. The values given above are thus only reasonable approximations.

An intersection is assumed to be bounded by 40 oxygen atoms resulting from four interconnecting channels at every intersection

$$\phi_i = \sum_{40} 4\epsilon_{ij} \left[\left(\frac{\sigma_m + d_o}{d_i + d_o} \right)^{12} - \left(\frac{\sigma_m + d_o}{d_i + d_o} \right)^{6} \right]. \tag{29}$$

The molecules are assumed to move along the center of the channels or intersections. Only intermolecular interactions of molecules which are within the same channel are taken into consideration. The intermolecular distances of molecule centers within a certain channel are set equal to the potential minimum ($=2^{1/6}\ \sigma_m$). One should appreciate that a simplifying spherical representation of the molecules was introduced. Actually, a more detailed representation of the potentials is possible, but this would have considerably increased the computer time for the large number of molecules taken considered.

Other potentials were determined by Snurr et al. [31]. Based on Eqs. (26) and (29) for the potential barriers, the probabilities, P, for the molecules to pass over these barriers are given by

$$P_a = 1 \quad \text{if RN} \leq \left(1 - \exp\left(\frac{-|\phi_i|}{kT} \right) \right), \tag{30}$$

$$P_a = 0 \quad \text{if RN} > \left(1 - \exp\left(\frac{-|\phi_i|}{kT} \right) \right), \tag{31}$$

$$P_b = 1 \quad \text{if RN} \leq \left(1 - \exp\left(\frac{-|\phi_i|}{kT} \right) \right), \tag{32}$$

$$P_b = 0 \quad \text{if RN} > \left(1 - \exp\left(\frac{-|\phi_i|}{kT} \right) \right), \tag{33}$$

where P_a and P_b are the probabilities of remaining on an active center and passing over a barrier at a channel

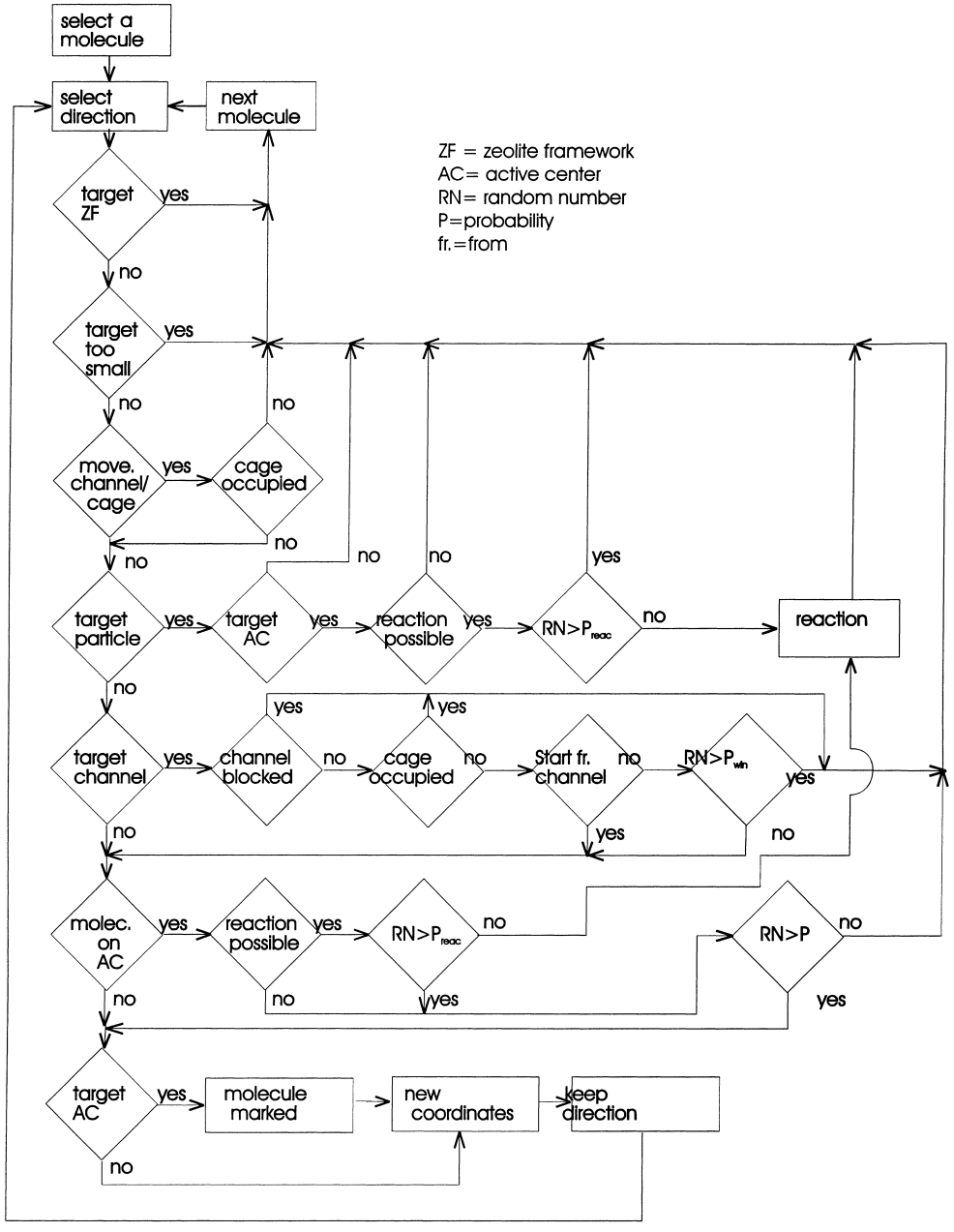

Fig. 4. MC program structure for the simulation of molecular movements.

crossing, respectively. RN represents a random number in the interval [0,1].

Tuning of an MC step to the real time of a physical system is still a problem. According to Kärger and Ruthven [14], a regular zeolite framework may be regarded as a sinusoidal potential field whose minima are preferred adsorption sites of the molecules. The harmonic oscillator is given by

$$\phi(x) = \frac{1}{2}\phi_0\left[1 - \cos\left(\frac{2\pi x}{L}\right)\right], \tag{34}$$

where ϕ_0 is the energy barrier between adjacent sites

or cages, and L represents the distance between two adsorption sites. The value of L was set to be equal to the value of α (=10 Å) in the paper written by Xiao and Wei [42]. The vibration frequency is

$$\nu = \left(\frac{\phi_0}{2mL^2}\right)^{1/2}, \tag{35}$$

where m is the mass of the molecule. The mean residence time on an active site, which is equal to the MC time step, is given by the reciprocal of the vibration frequency, ν, multiplied by a Boltzmann factor

$$\tau = \frac{1}{6\nu} e^{\phi_o/kT}. \tag{36}$$

The factor of 6 results from the six possible directions of movement. The stronger the interaction between the sorbate molecule and the zeolite framework, the more sensitive is the time interval to temperature changes. The order of magnitude of the time interval is in good agreement with MD results for the mean residence time on adsorption sites.

The self-diffusivities were obtained by means of the Einstein relation:

$$D_{\text{self}} = \lim_{t\to\infty} \frac{\langle(\bar{\mathbf{r}}(t) - \bar{\mathbf{r}}(0))^2\rangle}{6t} = \lim_{N\to\infty} \frac{\langle(\bar{\mathbf{r}}(t) - \bar{\mathbf{r}}(0))^2\rangle}{6N\tau}, \tag{37}$$

where N is the number of MC steps. The expressions in the numerators represent the mean square displacements. The distance between two adjacent lattice elements is correlated with the known dimensions of a channel intersection. There is thus no fitting parameter involved in this approach.

After initialization and 10 000 equilibrium steps, a production phase of 10 000 MC steps is started. The diffusivities were calculated every 100 MC steps and the average value after the production phase was finished.

The complete program structure of molecular movements is illustrated in Fig. 4. Some points should be stressed. It is checked whether an active center is occupied and whether a molecule on an active center can in principle undergo a chemical reaction. If, for an example, in a reaction scheme like A → B → C, C is on an active center, no reaction will take place.

4. Molecular dynamics simulations

In addition to the MC calculations, some MD simulations were also computed. In the past, a variety of MD computations have been carried out. A review of the topic has been presented by Demontis and Suffritti [8] and Theodorou et al. [34], for example.

One or two unit cells were employed in the present calculations. Data of the zeolite ZSM-5 lattice were taken from the literature [24]. Periodic boundary conditions were used. The calculations were done according to a microcanonical ensemble. For the integration of the equations of motion, a predictor–corrector algorithm proposed by Gear was used [10]. The algorithm is of fifth-order in time-step size, but is not stable for highly oscillatory problems. For methane pair, potentials between two methane molecules and between methane molecules and oxygen atoms were taken as [8]:

$$\phi_{CH_4-CH_4} = \frac{1.0992\times10^{11}}{r^{20}} - \frac{2.09865\times10^3}{r^6}\ (\text{kcal/mol}), \tag{38}$$

and

$$\phi_{CH_4-O} = \frac{2.28\times10^6}{r^{12}} - \frac{1.33\times10^3}{r^6}\ (\text{kcal/mol}), \tag{39}$$

where r is in Ångstroms.

Methane molecules are considered to be homogeneous spheres. Nowak et al. [23] have published potentials for water and methanol. The region of interacting forces is truncated to half the length of the smallest rectangle side (cut-off) to avoid undesirable symmetry effects. Methane–silicon interactions were dropped due to the reasons mentioned in the section about MC calculations. The self-diffusivities were determined by the Einstein formula (Eq. (37)). The diffusivities were calculated in two series.

MD calculations of methane diffusivities are presented in Table 2. Experimental results taken from the book written by Kärger and Ruthven [14] are given in Table 3. The calculated values correspond well with the experimental findings.

5. Results

As a lot of experimental data about self-diffusivities in silicalite have been published, the corresponding

Table 2
MD Simulations of methane diffusivities (n=number of particles per unit cell)

Simulation		T (K)	n	D (10^{-9} m^2/s)
Unit cell	1	300	12	8.88
Step size	1 fs	150	12	4.31
Equilibrium time	50 ps	200	12	9.28
Free simulation time	100 ps	250	12	8.56
Production time	200 ps	350	12	9.93
		400	12	11.3
		300	6	17.9
		150	6	10.4
Unit cells	2	700	24	17.4
Step size	0.1 fs	600	24	16.0
Equilibrium time	150 ps	500	24	12.0
Free simulation time	60 ps	400	24	11.0
Production time	1 ns	300	24	8.68

Table 3
Experimental results [14]

T (K)	167	169	202	221	290	298	304	446	451
D (10^{-9} m^2/s)	2.1	2.1	3.3	4.1	6.7	7.0	7.2	11.7	11.8

values were calculated by the above mentioned MC approach and in some cases by the MD method. In Fig. 5, the diffusivities of benzene in silicalite at various temperatures are presented. A kinetic diameter of 5.85 Å for benzene was taken.

The D_Z values are assigned to the straight channels and $D_{x/y}$ values to the zig-zag channels. As expected, the diffusivities in the straight channels are larger than those in the zig-zag channels. The values are in good agreement with experimental findings. The diffusivities are exponentially dependent on the temperature, i.e. an activated process. In Fig. 6, the concentration dependence of the diffusivities of methane in silicalite is illustrated. The sensitivity of the diffusivities to the Lennard-Jones length constant is also demonstrated. The agreement with experimental data is satisfactory. Figs. 7 and 8 demonstrate the diffusivities of methanol and water in silicalite at 300 K as a function of concentration. These molecules are important reactants in the MTO synthesis. The MC diffusivities found, agree qualitatively with NMR measurements. Although the detailed zeolite structure for the MC calculations is not taken into consideration, a rather good agreement between measurements and calcula-

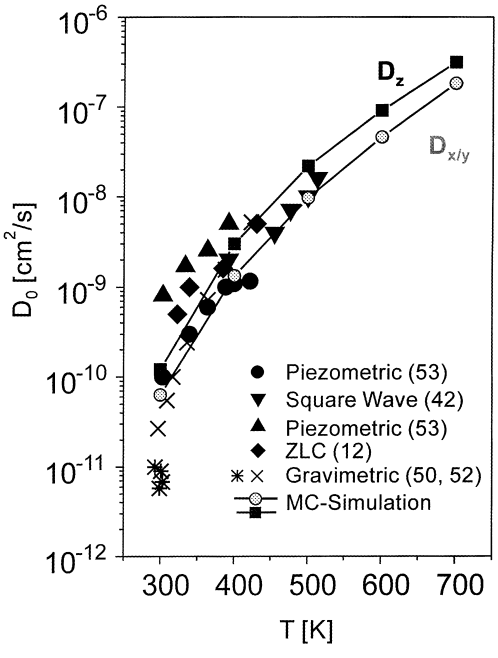

Fig. 5. Diffusivities of benzene in silicalite as a function of temperature.

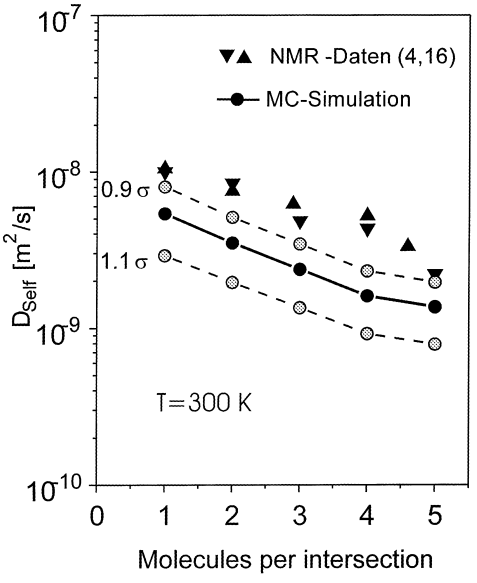

Fig. 6. Self-diffusivities of methane in silicalite as a function of concentration.

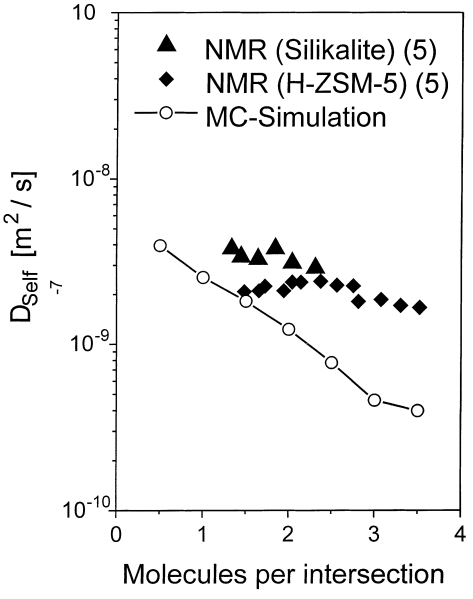

Fig. 8. Self-diffusivities of water in silicalite as a function of concentration.

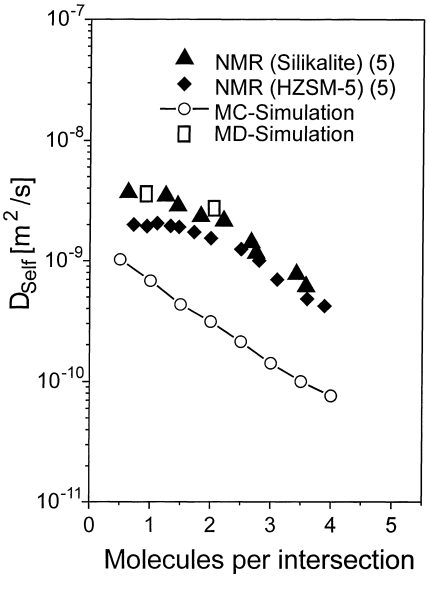

Fig. 7. Self-diffusivities of methanol in silicalite as a function of concentration.

tions could be obtained. Further results are presented by Hinderer and Keil [11].

For the simulations of the MTO synthesis, 4096 intersections of channels were taken. In the beginning, each intersection was randomly occupied by one methanol molecule on an average. At the outer surface, the concentration of methanol molecules was kept constant which corresponds to an adsorption equilibrium between the lattice and the adjacent phase. Methanol molecules which diffuse into the channels are replaced outside the lattice in every MC step. Reaction products which leave the lattice are removed and taken into consideration in the material balance. According to Theodorou and Wei [33], the average concentration of about one particle per intersection is a reasonable assumption for the conditions of the MTO synthesis. The reaction scheme was assumed to follow Eqs. (17)–(23). As molecule–molecule collisions have to be modeled, quantum chemical reaction paths should be taken. For some reaction steps, those calculations were done by van Santen [36] and other groups. In the present calculations, reaction probabilities were taken so that a concentration of reactants was obtained as was found by measurements in a Berty reactor. The stoichiometry in the reaction scheme has to be fulfilled. If a random number is smaller than the corresponding reaction probability, the reaction takes place. In a multicomponent mixture the molecule which has the largest residence time on an active center is taken

as a measure for the MC time step. After 750 000 MC steps, no significant change of the number of different molecules within the lattice was found. Collisions against the walls dominate. The diffusivities follow an exponential law as a function of temperature and the diffusivities decrease with increasing particle concentration. In Table 4, some comparisons between

Table 4
Diffusivities at 500°C in (m^2/s)

	One component	MTO synthesis
Water	1.69×10^{-8}	5.21×10^{-10}
Methanol	1.27×10^{-8}	3.89×10^{-10}
Paraffins	1.08×10^{-8}	6.62×10^{-9}

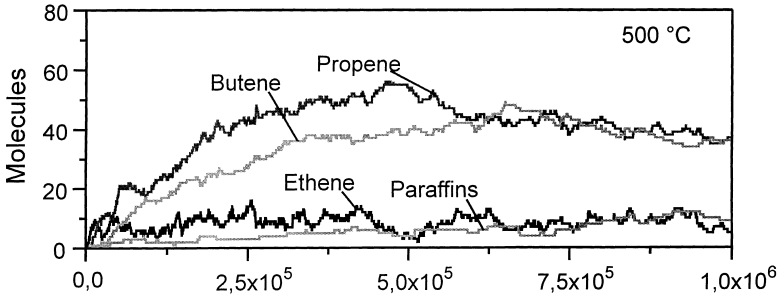

Fig. 9. Number of olefin and paraffin molecules within a lattice of 4096 intersection.

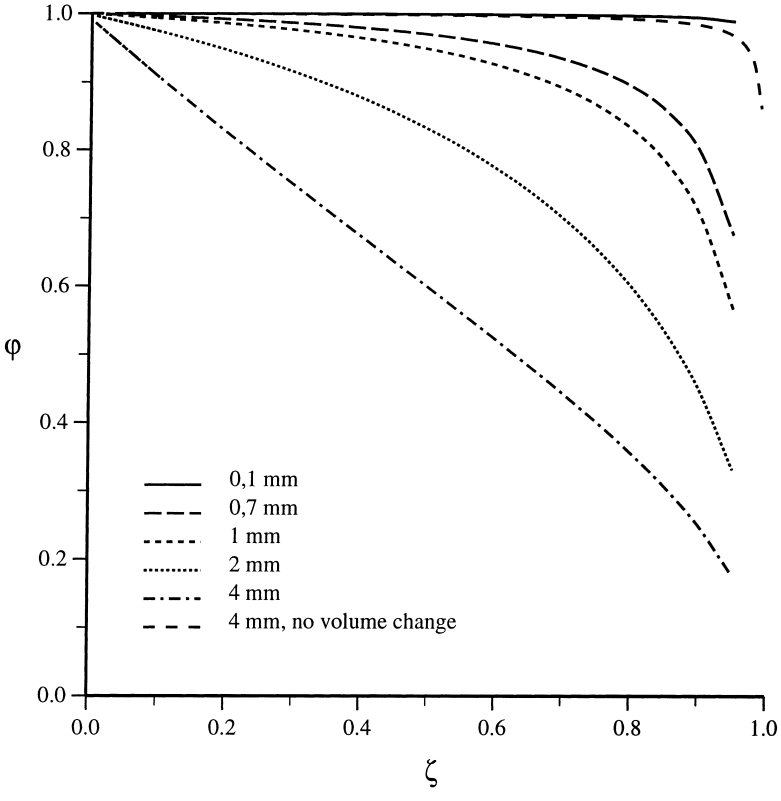

Fig. 10. Effectiveness factors of different composite catalyst pellets.

diffusivites of one-component systems and MTO synthesis conditions are presented. A multicomponent effect can be observed.

In Fig. 9, the composition of the reaction mixture as a function of MC steps is presented.

In Fig. 10, effectiveness factors as a function of particle size and zeolite fraction are given. For comparison, the effectiveness factors were also calculated by the formula of Ruckenstein [28]. This equation allows to calculate the effectiveness factor in the case of a first-order reaction with a constant volume. The calculated effectiveness factor of a large particle is also shown in Fig. 10. The values of the effectiveness factors calculated using the model in the present paper are substantially lower than those obtained by the model developed by Ruckenstein, which does not take the volume change into account.

6. Conclusions

A model for diffusion and reaction in ZSM-5 and composite catalysts for the MTO synthesis was developed. Diffusion and reaction in the zeolite particles were modeled with the aid of Monte Carlo calculations. The diffusivities agree well with experimental findings. Multicomponent effects of diffusivities could be observed. The volume change during the reaction was taken into account. It turned out that this effect influences the effectiveness factors of composite pellets considerably. The present model allows the employment of any common kinetics.

Improvements can be obtained by using more detailed quantum mechanical potentials which include vibrations, rotations, etc. Special molecular dynamics method for ''rare events'' would also lead to more exact results compared to MC approaches, especially for non-rigid zeolites. Instead of taking reaction rate constants from measurements, one could have used quantum mechanical calculations for some or all reaction steps. These calculations would have been very time consuming.

Acknowledgements

This work was financially supported by the Deutsche Forschungsgemeinschaft, Sonderforschungsbereich 238, the Max-Buchner-Forschungsstiftung and the Fonds der Chemischen Industrie. The authors are grateful to Prof. David Agar (Dortmund) for helpful discussions.

References

[1] M.P. Allen, D.J. Tildesley, Computer Simulation of Liquids, Oxford University Press, Oxford, 1987.
[2] H. Brauer, Mass Transfer Including Chemical Reactions, Verlag Sauerlaender, Frankfurt, 1971 (in German).
[3] D.W. Breck, Zeolite Molecular Sieves, Wiley, New York, 1974.
[4] N.Y. Chen, T.F. Degnan Jr., C.M. Smith, Molecular Transport and Reaction in Zeolites, VCH, New York, 1994.
[5] D.B. Dadyburjor, AIChE J. 28 (1982) 720.
[6] D.B. Dadyburjor, Ind. Eng. Chem. Fundam. 24 (1985) 16.
[7] J.W. Dean, D.B. Dadyburjor, Ind. Eng. Chem. Res. 28 (1989) 271.
[8] P. Demontis, G.B. Suffritti, in: C.R.A. Catlow (Ed.), Modelling of Structure and Reactivity in Zeolites, Academic Press, New York, 1992, pp. 79–132.
[9] B. Frank, K. Dahlke, G. Emig, E. Aust, R. Broucek, Microporous Mater. 1 (1993) 43.
[10] C.W. Gear, Numerical Initial Value Problems in Ordinary Differential Equations, Prentice-Hall, Englewood Cliffs, NJ, 1971.
[11] J. Hinderer, F.J. Keil, Chem. Eng. Sci. 51 (1996) 2667.
[12] J. Hinderer, F.J. Keil, Hung. J. Ind. Chem. 23 (1995) 207.
[13] R.L. June, A.T. Bell, D.N. Theodorou, J. Phys. Chem. 94 (1990) 1508.
[14] J. Kärger, D.M. Ruthven, Diffusion in Zeolites and other Microporous Solids, Wiley, New York, 1992.
[15] F.J. Keil, Chem. Eng. Sci. 51 (1996) 1543.
[16] R. Krishna, J.A. Wesselingh, Chem. Eng. Sci. 52 (1997) 861.
[17] R. Krishna, Gas Sep. Purif. 7 (1993) 91.
[18] S.H. Lee, E. Ruckenstein, Chem. Eng. Commun. 46 (1986) 43.
[19] E.J. Maginn, A.T. Bell, D.N. Theodorou, J. Phys. Chem. 99 (1995) 2057.
[20] E.J. Maginn, A.T. Bell, D.N. Theodorou, J. Phys. Chem. 100 (1996) 7155.
[21] H. Martin, Chem. Eng. Sci. 33 (1988) 913.
[22] E.A. Mason, A.P. Malinauskas, Gas Transport in Porous Media: The Dusty-Gas-Model, Elsevier, Amsterdam, 1983.
[23] A.K. Nowak, C.J.J. den Ouden, S.D. Pickett, B. Smit, A.K. Cheetham, M.F.M. Post, J.M. Thomas, J. Chem. Phys. 95 (1991) 848.
[24] D.H. Olson, G.T. Kokotailo, S.L. Lawton, J. Phys. Chem. 85 (1981) 2238.
[25] M.F.M. Post, Stud. Surf. Sci. Catal. 58 (1991) 391.
[26] L.V.C. Rees, Stud. Surf. Sci. Catal. 84 (1994) 1133.
[27] R.C. Reid, J.M. Prausnitz, B.E. Poling, The Properties of Gases and Liquids, McGraw Hill, New York, 1987.
[28] E. Ruckenstein, AIChE J. 16 (1970) 151.

[29] H. Schönfelder, J. Hinderer, J. Werther, F.J. Keil, Chem. Eng. Sci. 49 (1994) 5377.
[30] P.G. Smirniotis, E. Ruckenstein, Chem. Eng. Sci. 48 (1992) 585.
[31] R.Q. Snurr, A.T. Bell, D.N. Theodorou, J. Phys. Chem. 97 (1993) 13742.
[32] R. Taylor, R. Krishna, Multicomponent Mass Transfer, Wiley, New York, 1993.
[33] D. Theodorou, J. Wei, J. Catal. 83 (1983) 205.
[34] D.N. Theodorou, R.Q. Snurr, A. Bell, in: G. Alberti, T. Bein (Eds.), Comprehensive Supramolecular Chemistry, vol. 7, Pergamon Press, New York, 1996, pp. 507–548.
[35] R.A. van Santen, D.P. de Bruyn, C.J.J. den Ouden, B. Smit, Stud. Surf. Sci. Catal. 58 (1991) 317.
[36] R.A. van Santen, G.J. Kramer, Chem. Rev. 95 (1995) 637.
[37] P.R. van Tassel, H.T. Davis, A.V. McCormick, Mol. Phys. 73 (1991) 1107.
[38] P. Varghese, E.E. Wolf, AIChE J. 26 (1980) 55.
[39] A.F. Voter, J. Chem. Phys. 106 (1997) 4665.
[40] J.G. Wang, Y.W. Li, S.Y. Chen, S.Y. Peng, Catal. Lett. 26 (1994) 189.
[41] J.G. Wang, Y.W. Li, S.Y. Chen, S.Y. Peng, Zeolites 15 (1995) 288.
[42] J. Xiao, J. Wei, Chem. Eng. Sci. 47 (1992) 1123.